PROCEEDINGS OF SCIENCE

Estimation of charm production cross section in the forward kinematic cone at energies $E_{Lab} \sim 75$ TeV according to the high mountain experiment with two-storey XREC

A.S.Borisov*, **V.G.Denisova, Z.M.Guseva, E.A.Kanevskaya, M.G.Kogan, A.E.Morozov, V.S.Puchkov, S.E.Pyatovsky, G.P.Shoziyoev, M.D.Smirnova, A.V.Vargasov**

P.N.Lebedev Physical Institute of the Russian Academy of Sciences, Moscow, Russia
E-mail: asborisov55@mail.ru

V.I.Galkin, S.I.Nazarov

M.V.Lomonosov Moscow State University, Moscow, Russia

R.A.Mukhamedshin

Institute for Nuclear Research of the Russian Academy of Sciences, Moscow, Russia

One-year exposition data on absorption of high-energy cosmic ray hadrons with energies of tens of TeV in two-storey X-ray emulsion chamber (XREC) with large air gap (~ 2.2 m) are presented. The experiment was carried out at the Tien Shan High Mountain Research Station located at the altitude of 3340 m a.s.l. It is shown that the abnormal behavior of the hadron absorption curve, which was formerly observed in some cosmic ray experiments with deep lead calorimeters, can be accounted for by assuming a rapid growth of charmed particle production efficiency in the forward cone with increasing energy. The experimental results of both the two-storey XREC exposition and earlier expositions of homogeneous lead calorimeters are compared with simulation data calculated on the basis of a phenomenological hadronic interaction model (code FANSY 1.0) implementing quark-gluon string theoretical approaches and assuming various charm production cross section parameters. A preliminary result of charm production cross section in the forward cone at energy $E_{Lab} \sim 75$ TeV is discussed. Particularly, the result is compared with those of collider experiments (RHIC and LHC) obtained for kinematic central region characterizing by relatively low pseudorapidities.

The 34th International Cosmic Ray Conference,
30 July- 6 August, 2015
The Hague, The Netherlands

*Speaker.

PoS(ICRC2015)332

1. Introduction

A slowing down of the absorption of high energy (tens of TeV) hadron cascades was observed at the Tien Shan High-Mountain Research Station (TSS) in extensive air shower (EAS) experiments with the Big Ionization Calorimeter (BIC) of 36 m^2 which contained lead absorber of 850-g/cm^2 thick [1, 2]. To explain the effect, a hypothesis of existence of a so-called long-flying cosmic ray (CR) component was introduced [2, 3]. An abnormally weak absorption of hadrons was also soon observed [4] in the *Pamir* experiment while exposing deep uniform XRECs with lead absorber 110 cm thick. In the range of $t < 70$ radiation lengths, the absorption curve obeys the conventional exponential law with index $\lambda_{abs}^{(1)} = 200 \pm 5$ g/cm^2. However, at larger depths $t > 70$ r.l., the absorption length of hadrons in lead changes and becomes as high as $\lambda_{abs}^{(1)} = 340 \pm 80$ g/cm^2.

It was soon suggested [5, 6] that both phenomena, i.e., excess ionization in the hadron calorimeter and hadron excess in the deep uniform XREC, result from high values of the cross section of production of leading charm particles (D mesons and Λ_c^+ hyperons) at energies $E_{Lab} \sim 50$ TeV.

To prove this hypothesis, a dedicated experiment was proposed [7] which employs a two-storey XREC with a large air gap between two vertically separated lead blocks of the chamber.

The main idea of the experiment is to allow charmed particles to decay effectively within a gap of width $H \simeq c\tau\gamma = c\tau \cdot E/m \approx 2.5$ m emitting $e^{\pm}$ particles and γ-rays within leptonic and semileptonic decay modes. Here τ is the life-time of D mesons, γ, E and m are their Lorentz factor, energy and mass respectively. The emitted electromagnetic (EM) particles will generate electromagnetic cascades (EMC) in the lower lead block and will thus manifest themselves as a bump on the absorption curve while high energy EM particles produced by CRs above the chamber will be effectively screened out by the upper lead block. The magnitude of the bump should obviously correlate with the value of charm production cross section. Such experiments have been recently carried out at the TSS and are now going on at the Pamirs.

This work presents an analysis of experimental data on the absorption of CR hadrons obtained during a one year exposure (2007 – 2008) of the two-storey XREC at TSS. Experimental and simulated data are compared assuming various values of charm production cross section.

2. Design and some specific features of the two-storey XREC

To construct a two-storey XREC with a large air gap, we take advantage of specific features of a two-storey laboratory building at the Tien Shan Station (TSS) located at an altitude of 3340 m a.s.l. (700 g/cm^2). The XREC, exposed during $2007 - 2008$, consisted of the upper and lower blocks with areas of 48 m^2 and 32 m^2, respectively, and 2.16 m air gap between them (Fig. 1).

The upper block of the chamber consists of a so-called Γ-block (containing three layers of X-ray films under 3.5, 5.0 and 6.5 cm of lead) and conventional Pb-block separated by two rows of ionization chambers and a 1.5 cm thick lead absorber between them. The Pb-block has 23 lead layers. The thickness of the first lead layer is 2 cm, while other lead layers are each 1 cm thick. In the central part of the Pb-block, the lead layers are interleaved with X-ray films covering only 12 m^2 of its total area. Thus the total depth of the lead absorber in the upper block is 32 cm. Until now only the 1st, 2nd, 4th, 9th, 10th, 14th, 20th and 2lst layers of X-ray films of the Pb-block have been treated carefully.

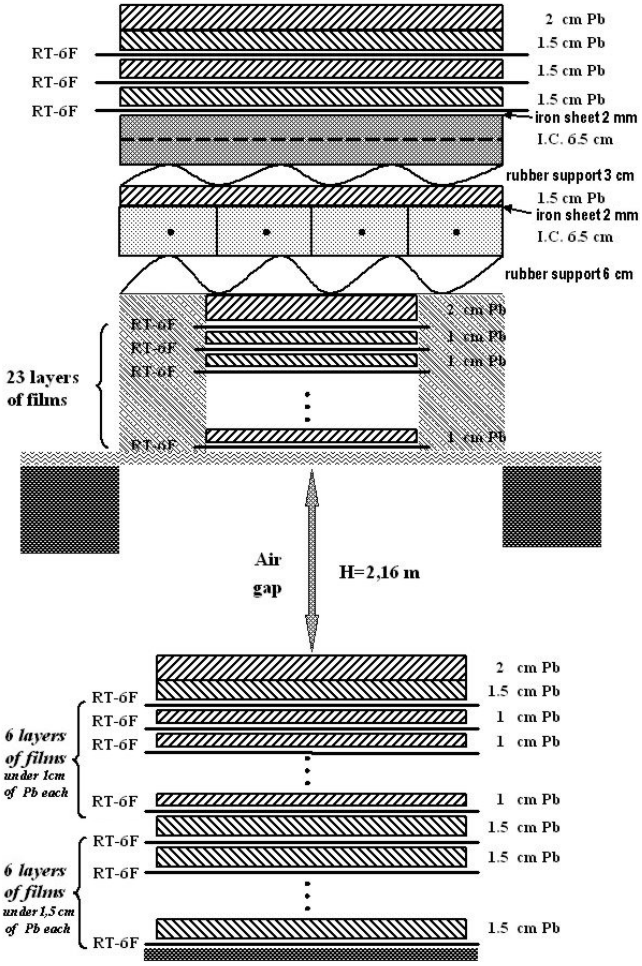

Figure 1: Profile of the two-storey XREC with 2.16-m air gap and 48/32-m^2 area exposed at the TSS.

The lower block of the two-storey XREC includes 13 layers of X-ray films. The first layer is placed under 3.5 cm of lead; the next six X-ray film layers are separated by 1 cm of lead, and the last six film layers are separated by 1.5 cm of lead. Until now only the first four and 6th, 7th and 12th X-ray film layers of the lower block have been treated.

The CR EM component incident on the XREC is almost completely absorbed in the Γ-block. Thus the hadron-induced showers are the only source of darkness spots observed in the Pb-block. The estimated threshold energy of the recorded hadron-induced cascades is $\sim 6-8$ TeV.

Hadron-induced showers originating in the upper block practically vanish in the air gap of the two-storey XREC. Only penetrating hadrons and successive hadronic interactions in the lead absorber of the lower block can produce darkness spots on X-ray films placed in the lower block. Therefore, we should observe a drastic decrease of the darkness spot intensity in the first six centimeters of the lower block if it were not for charm production. Charm particles, produced in the upper block, effectively decay in the air gap, partially emitting EM particles which should generate EMCs in the lead absorber of the lower block.

3. Simulation of the experiment and the XREC response

Simulations of both experiments, i.e., with the two-storey XREC and deep homogeneous lead XREC, were carried out assuming that the incident CR hadrons at mountain altitudes are mainly represented by nucleons and pions with energies $E_h \geq 20$ TeV produced by PCR protons and nuclei. It was assumed that relative fractions of incident nucleons and pions are 60% and 40% while indices of their power energy spectra are -3.10 and -3.22, respectively. Besides, we take into account, if the other is not mentioned explicitly, angular distributions of incident particles found in the XREC experiments, i.e., $dN/d\theta \sim \cos^6(\theta)$.

Nuclear-EM cascades (NEC) produced by incident hadrons in XREC were simulated with the software package ECSim2.0 [8], which allows to calculate the XREC response taking into account the exact experimental technique employed in the *Pamir* experiment including processing and measurement of darkness spots produced on X-ray films.

To generate nucleon-lead and pion-lead interactions accounting for the production of charm hadrons and their subsequent decay in the air gap with the emission of $e^{\pm}$ and γ-rays, the FANSY 1.0 model [9] was used and incorporated in the ECSim 2.0 package. In many features it is close to the QGSGET II model. However, in pp interactions x_F spectra of secondary particles including charmed ones appeared to be too soft as compared to the LHC data.

To make results of the experiment more robust to experimental errors and fluctuations in NEC development taking into account limited experimental statistics, we treated not only reconstructed individual cascades but also separate darkness spots as we observe them at each film layer, i.e., quite independently from layer to layer. This procedure increases the statistics of the experimental data being analyzed and strongly diminishes the experimental ambiguities related to the rather complicated procedure of reconstruction of cascades recorded with multi-layered XRECs.

Results simulated with the ECSim2.0@FANSY 1.0 code for the Tien Shan two-storey XREC are presented in Figs. 2 and 3. A dependence of darkness spot number per one X-ray film and per one incident particle on the observation level t expressed in lead absorber depth is plotted in Fig. 2 for three cases of charm production cross section in the forward-cone region ($x_{Lab} > 0.1$): $\sigma^{fragm}_{h\to charm} \sim 0; \sim 6; \sim 8$ mb/nucleon.

As follows from Fig. 2, in the case of negligible charm-production cross section $\sigma^{fragm}_{h\to charm} \sim 0$, there is a drastic fall of the spot number in the initial layers of X-ray films in the XREC's lower block just after the air gap (or after the layer corresponding to 32 cm of lead absorber in the plotted distribution). Then we observe a gradual restoration of distribution points to the same exponential dependence as observed in the upper block of the XREC. Such a behaviour of the darkness spot distribution is explained by a lead-air-lead transition effect taking into account the large air gap and specific features of hadron cascades in lead absorber determined by a large difference in values of the mean free path for nuclear interaction ($\lambda^{\pi-Pb}_{int} \approx 10.5$ cm) and radiation length ($X_0 \approx 0.56$ cm) in lead.

However, at $\sigma^{fragm}_{h\to charm} \sim 6-8$ mb/nucleon, we observe (Fig. 2) a bump on the darkness spot distribution at initial layers of X-ray films in the lower block due to the appearance of EMCs generated via decays of charmed particles in the air gap. The relative amplitude of this bump increases with increasing $\sigma^{fragm}_{h\to charm}$ that makes it possible to measure the charm production cross section at $x_{Lab} \gtrsim 0.1$ in experiments with two-storey XRECs. This bump appears to be more pronounced with

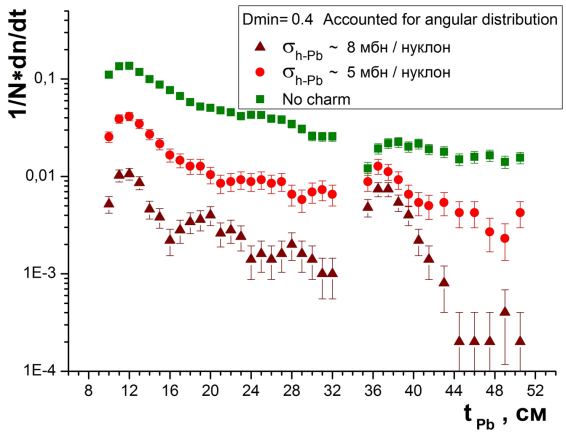

Figure 2: Distributions of darkness spots with optical densities D > D_{min}=0.4 vs. observation lead depth t simulated at three charm production cross sections $\sigma^{fragm}_{h\to charm}$: ~ 0; ~ 6; ~ 8 mb/n.

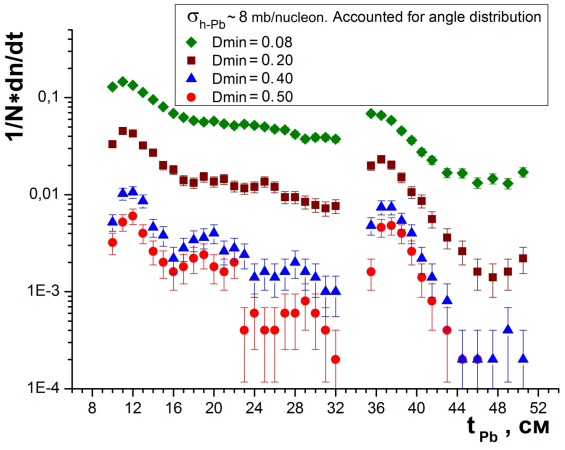

Figure 3: Simulated distributions of observed darkness spots vs. observation lead depth t at different optical density thresholds D_{min} ($D_{min} = 0.08, 0.2, 0.4, 0.5$).

increasing the darkness threshold, D_{min}, for observing the spots (Fig. 3). In addition we observe some shifting of the position of the bump to the larger depth with increasing D_{min}.

We applied the same ECSim2.0@FANSY 1.0 code with high values of charm production cross sections for simulation of the experiment with deep uniform lead XRECs 110-cm thick which were exposed at the Pamirs in the mid 1980s. Simulation results on the distribution of origin points of hadron cascades in *Pamir*'s XREC assuming two values of charm production cross section $\sigma^{fragm}_{h\to charm}$, namely, ~ 5 and ~ 8 mb/nucleon, are presented in Fig. 4. One can see that accounting for charm production leads to an increase of the absorption length of hadron cascades just from the very top of the absorber, so the distribution of the origin points of hadron cascades can be approximated by one exponential law for the whole depth of the absorber. Besides, the slope of the absorption curves strongly depends on the value of the charm production cross section.

4. Comparison of experimental and simulated data

The preliminary experimental distribution of darkness spots observed in the Tien Shan two-storey XREC over observation lead absorber depth, t, is plotted in Fig. 5. To compare experimental and simulated data, the experimental distribution was normalized to the simulated one calculated with $\sigma^{fragm}_{h\to charm} \sim 6$ mb/nucleon at a point corresponding to 10-cm lead depth in the XREC's upper block.

Note that simulated distributions were obtained on assumption that the observation threshold of the darkness spots $D_{min} = 0.4$, where D is the spot optical density. According to our preliminary measurements of spot optical densities, this D_{min} value is close to the experimental threshold although it should be increased by $\sim 35\%$.

One can see from Fig. 5 that the simulated distribution corresponding to the case, when $\sigma^{fragm}_{h\to charm} \sim 6$ mb/nucleon, fits the experimental data rather well unless you consider some shift in the position of the experimental bump to larger observation depths as compared with simulated

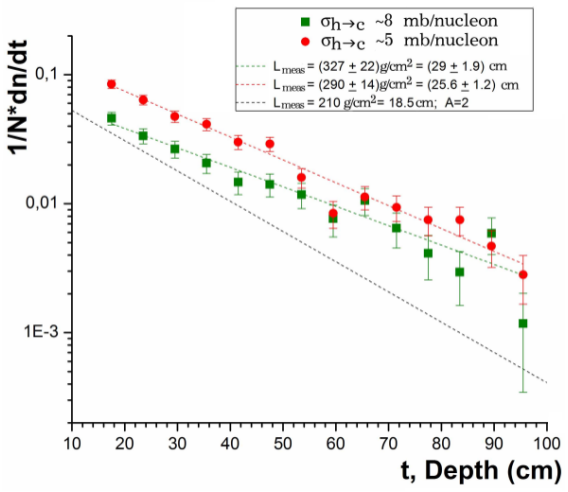

Figure 4: Simulated distributions of hadron-cascade origin points in homogeneous lead XREC at $\sigma^{fragm}_{h\to charm} \sim 5$ and ~ 8 mb/n. Fractions of incident nucleons and pions are 60% and 40%, respectively (optical density threshold is $D_{min} = 0.08$). Lines show $exp((-t/L_{meas}) - A$ dependencies.

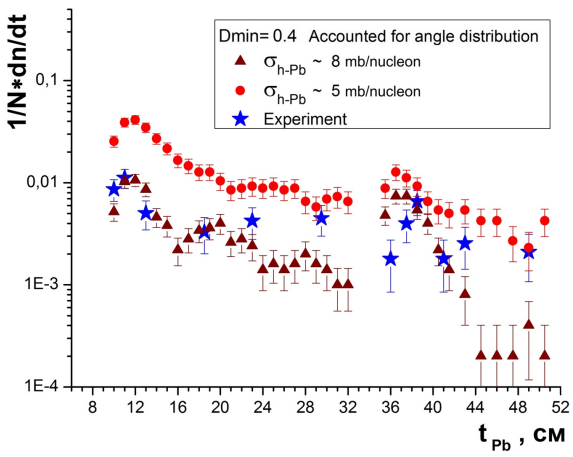

Figure 5: Lead depth dependence of number of darkness spots in the Tien Shan two-storey XREC: experimental data (number of darkness spots per X-ray film) (blue stars) and simulation results with $\sigma^{fragm}_{h\to charm} \sim 5$ and ~ 8 mb/n at optical density threshold $D_{min} = 0.40$.

distributions. As shown in Fig. 3 the bump position is sensitive to the optical density threshold D_{min} for observation of the darkness spots, i.e., the bump slightly shifts to the larger lead depths with increasing D_{min}. Thus the observed discrepancy between the experimental data and simulated one can be, partially, explained by higher energy threshold for hadron detection in our experiment.

The same approach for explaining the abnormal behaviour of hadron absorption in lead was applied to analyze experimental data obtained with the deep homogeneous lead XRECs 110 cm thick exposed at the Pamirs [4]. The experimental distribution of cascade origin points for hadrons with $E_h^{(\gamma)} \gtrsim 6.3$ TeV is presented in Figs. 6 and 7.

Experimental data are compared with simulated ones calculated with the ECSim2.0@FANSY 1.0 code on the assumption of two different values of charm production cross section, namely, $\sigma^{fragm}_{h\to charm} \sim 5$ mb/n (Fig. 6) and $\sigma^{fragm}_{h\to charm} \sim 8$ mb/n at $x_{Lab} > 0.1$ (Fig. 7). Fractions of incident nucleons and pions are 60% and 40%, respectively. As follows from these figures, the data set, simulated with $\sigma^{fragm}_{h\to charm} \sim 8$ mb/n, fits the experimental data well enough. However, simulated distributions do not allow us to distinguish two different components in the experimental hadron flux which obey different exponentials [4].

5. Discussion

Recently ALICE, LHCb and ATLAS collaborations have measured inclusive transverse momentum spectra of open-charm mesons in proton-proton collisions at $\sqrt{s} = 2.76$ and 7 TeV. These results are very interesting from the theoretical point of view due to the highest collision energy ever achieved in accelerator experiments and due to a unique rapidity acceptance of the detectors. Especially, results from the middle rapidity region $2 < \eta < 4$, obtained by the LHCb, as well as

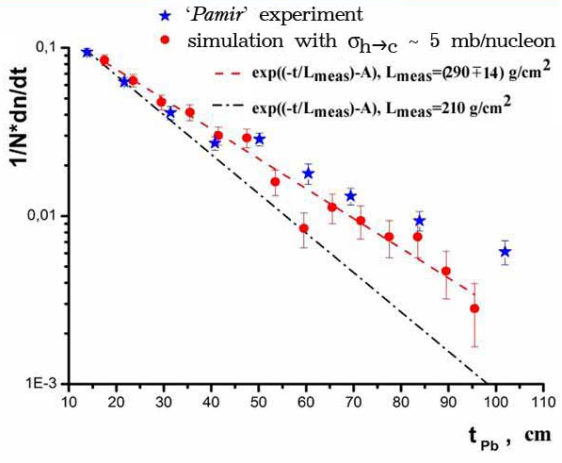

Figure 6: Distributions of hadron-cascade origin points produced in lead XREC if $\sigma^{fragm}_{h\to charm} \sim 5$ mb/n.

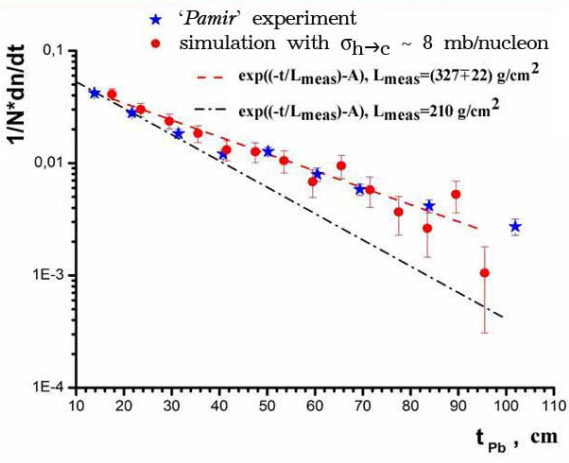

Figure 7: The same distribution as in Fig. 6 but on assumption of $\sigma^{fragm}_{h\to charm} \sim 8$ mb/n.

ATLAS data from central pseudorapidity range $\eta < 2.1$ can improve our understanding of pQCD production of heavy quarks (see, e.g., [10, 11, 12]).

Unfortunately, particles, produced in the most forward cone of phase space with high values of pseudorapidities η (i.e., in the so-called fragmentation region of a projectile particle), are practically unobservable by colliders due to their specific constructional traits (finite dimension of the acceleration pipe which hinders placing detectors close to the collision axis). On the contrary, CR experiments with fixed target make it possible to investigate the fragmentation region of projectile particles, i.e., $x_{Lab} \gtrsim 0.1$, where the behaviour of charm production with energy could be different from that observed in the central range. In any case, CR experiments could give some complementary information to collider data.

Significance of the forward region greatly increases with interaction energy, so that it begins to play a key role at the primary energies under investigation (for instance, at the energy $E_0 \sim 10^{17}$ eV almost 90% of the collision energy is released in the region $\eta \geq 5$).

First results of rapid growth of charm hadroproduction cross sections with energy in the mid rapidity range were presented by the STAR/RHIC Collaboration [13] and later confirmed by the PHENIX Collaboration [14]. A strong energy dependence of the total charm production cross section was revealed: $\sigma_{pp\to c\bar{c}} \sim E^{0.8}$.

The total charm production cross section at $\sqrt{s} = 2.76$ and 7 TeV was evaluated, rather than measured, by extrapolating from the central rapidity range to the full phase space using theoretical models. The experimental data are, first, fitted with simulations performed within the framework of perturbative-QCD (pQCD) approaches accounting for Next-to-Leading Order (NLO) corrections and, then, the measured cross section are scaled by the ratio of the total cross section over the cross section in the experimentally covered phase space calculated using the NLO pQCD technique.

Results obtained at $\sqrt{s} = 2.76$ and 7 TeV by the ALICE, ATLAS and LHCb Collaborations are in fair agreement [11] with each other: $\sigma^{tot}_{pp\to c\bar{c}}(2.76\text{ TeV}) = 4.8 \pm 0.8(stat)^{+1.0}_{-1.3}(syst.)$ mb, $\sigma^{tot}_{pp\to c\bar{c}}(7\text{ TeV}) = 8.5 \pm 0.5(stat)^{+1.0}_{-2.4}(syst.)$ mb.

Taking into account rather large uncertainties of the applied procedure, one can conclude that

CR experiments provide high energy physicists with complementary information on the charm hadroproduction mechanism.

As follows from comparison of results obtained in collider and CR experiments, cosmic ray values seem to be too high. We believe that accounting for high energy incident muons (including so-called prompt muons originating via the decay of charm particles) and an implementation of a harder spectra of secondary particles in the FANSY 1.0 model in accordance with recent LHC results will decrease the value of the charm production cross section. A possible contribution of methodical errors into the experimental data must also be analyzed in detail.

6. Conclusion

The analysis of experimental data obtained in two high altitude experiments with a two-storey XREC and a deep uniform XREC shows that an abnormally weak absorption of hadrons in the thick lead absorber can be explained with a rapid increase of forward-cone charm production cross section $\sigma^{fragm}_{hp\to charm}$ with energy up to such high values as $6-8$ mb/nucleon at energies $\langle E_h^{Lab}\rangle \sim 75$ TeV. However, the available experimental statistics do not allow us to exclude other possible hypotheses, for instance, the existence of some additional long-flying CR component like strangelets which can also contribute to the observed effects and, in particularly, result in the bending of the hadron absorption curve [4].

References

[1] V.S. Aseikin et al., *Izvestiya of AN of USSR*, ser. fiz., No 5, p. 998 (1974).

[2] S.I. Nikolsky, E.L. Feinberg, V.P. Pavluchenko, V.I. Yakovlev. Preprint FIAN, N 69 (1975).

[3] I.M. Dremin, V.I. Yakovlev, *Topics on Cosmic Rays. 60th Anniversary of C.M.G. Lattes*. Campinas, 1984, V. 1, P. 122.

[4] Collaboration of Experiment PAMIR, *Izv. AN USSR*, Ser. fiz., 1989, V. 53, No. 2, P. 277.

[5] V.I. Yakovlev, *Proc. 24th ICRC*, Rome (1995) v. 1, p. 446.

[6] I.M. Dremin, D.T. Madigozhin, V.I. Yakovlev, *Proc. 21st ICRC*, Adelaide, 1990, V. 10, P. 166.

[7] L.G.Sveshnikova, O.P.Strogova, *Proc. 23rd ICRC*, Calgary (1993) v. 4, p. 33.

[8] A.S. Borisov, V.G. Denisova, V.I. Galkin et al, *Proc. 30th ICRC*, Merida (2007) v. 4, 593

[9] R.A. Mukhamedshin, *Eur.Phys.J.* C60 (2009) 345

[10] B. Abelev et al. (The ALICE Collaboration), *JHEP* 01 (2012) 128; The ALICE collaboration, [CERN-PH-EP-ALICE-2012-069]; [nucl-ex/1203.2160v4]; [hep-ex/1205.4007v2]

[11] The LHCb Collaboration, LHCb-CONF-2010-013

[12] The ATLAS Collaboration, ATLAS-CONF-2011-017

[13] A. Tai, *J. Phys.* G 30 (2004) S809; The STAR collaboration. [nucl-ex/1204.4244v3]

[14] S. Kelly, *J. Phys.* G 30 (2004) S1189.